

# Optically Controlled Extraordinary Terahertz Transmission of Bi<sub>2</sub>Se<sub>3</sub> Film Modulator

Junhu ZHOU<sup>1†</sup>, Tong ZHOU<sup>2†</sup>, Dongsheng YANG<sup>1†</sup>, Zhenyu WANG<sup>2,3\*</sup>,  
Zhen ZHANG<sup>4</sup>, Jie YOU<sup>2,3</sup>, Zhongjie XU<sup>1</sup>, Xin ZHENG<sup>2,3</sup>, and Xiang-ai CHENG<sup>1,2</sup>

<sup>1</sup>College of Advanced Interdisciplinary Studies, National University of Defense Technology, Changsha 410073, China

<sup>2</sup>State Key Laboratory of High Performance Computing, National University of Defense Technology, Changsha 410073, China

<sup>3</sup>National Innovation Institute of Defense Technology, Academy of Military Sciences PLA China, Beijing 100010, China

<sup>4</sup>State Key Laboratory of Laser Interaction with Matter, Northwest Institute of Nuclear Technology, Xi'an 710024, China

<sup>†</sup>These authors contributed equally to this work and are both first authors

\*Corresponding author: Zhenyu WANG      Email: oscarwang2008@sina.com

**Abstract:** Standing on the potential for high-speed modulation and switching in the terahertz (THz) regime, all-optical approaches whose response speeds mainly depend on the lifetime of nonequilibrium free carriers have attracted a tremendous attention. Here, we establish a novel bi-direction THz modulation experiment controlled by femtosecond laser for new functional devices. Specifically, time-resolved transmission measurements are conducted on a series of thin layers Bi<sub>2</sub>Se<sub>3</sub> films fabricated straightforwardly on Al<sub>2</sub>O<sub>3</sub> substrates, with the pump fluence range from 25 μJ/cm<sup>2</sup> to 200 μJ/cm<sup>2</sup> per pulse. After photoexcitation, an ultrafast switching of THz wave with a full recovery time of ~10 ps is observed. For a longer timescale, a photoinduced increase in the transmitted THz amplitude is found in the 8 and 10 quintuple layers (QL) Bi<sub>2</sub>Se<sub>3</sub>, which shows a thickness-dependent topological phase transition. Additionally, the broadband modulation effect of the 8 QL Bi<sub>2</sub>Se<sub>3</sub> film is presented at the time delays of 2.2 ps and 12.5 ps which have a maximum modulation depth of 6.4% and 1.3% under the pump fluence of 200 μJ/cm<sup>2</sup>, respectively. Furthermore, the absorption of α optical phonon at 1.9 THz shows a time-dependent evolution which is consistent with the cooling of lattice temperature.

**Keywords:** Ultrafast optics; topological insulator; ultrafast photonic devices

---

Citation: Junhu ZHOU, Tong ZHOU, Dongsheng YANG, Zhenyu WANG, Zhen ZHANG, Jie YOU, Zhongjie XU, Xin ZHENG, and Xiang-ai CHENG, "Optically Controlled Extraordinary Terahertz Transmission of Bi<sub>2</sub>Se<sub>3</sub> Film Modulator," *Photonic Sensors*, 2019, 9(3): 268–276.

---

## 1. Introduction

Benefiting from the breakthrough of ultrafast lasers and semiconductors in recent decades, the understanding of THz frequency has been dramatically deepened especially in its source and

detection. Bright prospects in myriad aspects such as imaging [1], communication [2], and sensing [3] have been revealed, thus attracting increasing research efforts. Considering many basic functional devices in other wave bands cannot be well transplanted to the THz regime, tunable devices

operating in the THz regime and preferably working at room temperature are still urgently desired. Conventionally, the subwavelength periodical structure with noble metals, so-called metamaterial/metasurface, which can overcome the limitations of weak electromagnetic response of natural materials with THz wave, is once regarded as the promising alternative to the THz optoelectronic and plasmonic devices [4]. However, their dielectric properties can only be slightly engineered in metal [5]. In comparison, hybridized metamaterials with tunable semiconductors (e.g., Si, GaAs, and perovskite) have shown remarkable modulation effects as well as the flexibility in selecting the modulation process, including the optical, electrical, thermal, or mechanical method [6, 7]. In view of this, one interesting and intriguing research routine is to construct suitable material systems with significant optoelectronic and plasmonic characteristics, in order to realize effective controllability of electromagnetism.

Topological insulator (TI) is a new quantum phase of matter [8, 9]. Owing to the presence of Dirac cone in the surface band structure, the topological surface state (TSS) exhibits a typical metal property, while the bulk state remains an ordinary semiconductor behavior [10]. The natural coexistence of metallic and semiconducting behaviors of TIs without the artificial progress as well their stable surface with strong antioxidant property are remarkable advantages for novel tunable THz devices [11–14]. Though there is an intrinsic distinction in the photoconductivity response mechanism between the bulk state and the metallic TSS, Bi<sub>2</sub>Se<sub>3</sub> has shown significant potentials for the applications of bi-direction THz modulators.

## 2. Methods

In this work, we demonstrate an ultrafast photoactive switching of Bi<sub>2</sub>Se<sub>3</sub> films layered from

2 quintuple layers (QL), 4 QL, and 8 QL to 10 QL by using optical-pump-THz-probe (OPTP) spectroscopy. A Spectra Physics Ti: Sapphire regenerative amplifier system which can produce 800 nm pulses (1 kHz, ~100 fs) acts as a light resource. The pump pulse of 400 nm is generated by the second harmonic generation. A broad band THz probe in the range of 0.1 THz to 2.1 THz is employed in this study. Two <1 1 0> ZnTe crystals are used to generate and detect THz fields via optical rectification and electro-optic sampling. Under photoexcitation [see Fig. 1(d)], the photoinduced suppression and enhancement of transmitted THz radiation are observed simultaneously, showing different responses when compared with their semiconductor counterparts. In the case of 8 QL sample, which has different carriers in bulk state and TSS, the distinguished THz switching behavior (i.e., over 8% modulation depth) is presented within 5 ps under a considerably low pump fluence of 200  $\mu\text{J}/\text{cm}^2$ . Additionally, the broadband photoinduced switching is realized but not limited from 0.1 THz to 2.0 THz. Especially for  $\alpha$  optical phonon with the resonant frequency of 1.9 THz, a time-evolved suppression effect is found on THz modulation, which provides an additional degree of freedom for spectral modulation. Furthermore, it is possible to achieve the ultrafast THz switching within 5 ps via the superimposed response from the spatial thermal diffusion effect [15]. Importantly, the various species of quantum states including Dirac electrons and semiconductor-like bulk states make possible for TIs' applications in ultrafast photoactive switches and dynamic manipulation of THz waves.

## 3. Results and discussion

### 3.1 Growth and characterization of Bi<sub>2</sub>Se<sub>3</sub> films

Bi<sub>2</sub>Se<sub>3</sub> films are grown on the sapphire substrate by a customized molecular beam epitaxy (MBE) under a base vacuum of  $\sim 1.0 \times 10^{-10}$  Torr. The growth

is monitored *in situ* by the reflection high-energy-electron diffraction (RHEED, RH 30 OM) pattern, with a growth speed stable at about 0.25 QL/min. Thus, we can accurately change the layer numbers of Bi<sub>2</sub>Se<sub>3</sub> films by tuning its growth time. The RHEED pattern is presented in Fig. 1(a), indicating that the lattice constant of our epitaxy Bi<sub>2</sub>Se<sub>3</sub> is 4.194 Å, which is consistent with the reported lattice constant of rhombohedral Bi<sub>2</sub>Se<sub>3</sub> (4.140 Å). Additionally, the film quality is further confirmed by atomic force microscope (AFM, Innova) [Fig. 1(b)]. Overall, our films exhibit a good flatness over a relatively large detection field range.

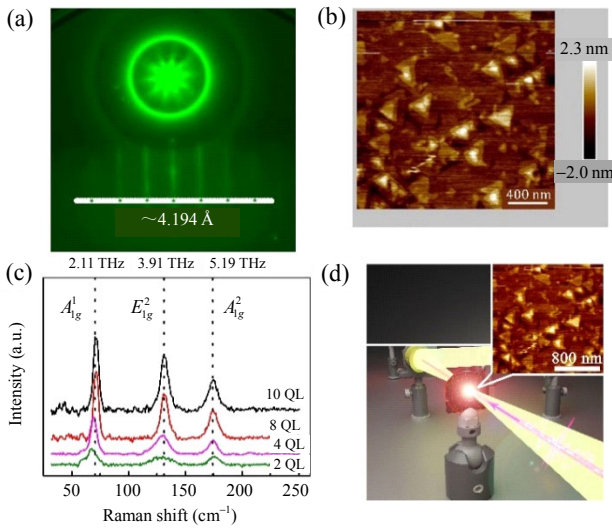


Fig. 1 Characterization of Bi<sub>2</sub>Se<sub>3</sub> films by: (a) RHEED pattern, (b) AFM, (c) Raman spectroscopy, and (d) schematic diagram of photoactive switching of THz wave with the Bi<sub>2</sub>Se<sub>3</sub> sample.

To further characterize the Bi<sub>2</sub>Se<sub>3</sub> films, the Raman spectroscopies of various layers of Bi<sub>2</sub>Se<sub>3</sub> samples are measured, as illustrated in Fig. 1(c). From this figure, three characteristic peaks are identified at 70.9 cm<sup>-1</sup>, 131.2 cm<sup>-1</sup>, and 174.3 cm<sup>-1</sup>, with the corresponding central frequencies of phonon modes to be 2.11 THz, 3.91 THz, and 5.19 THz. This result is in good agreement with the out-of-plane vibrational modes  $A_{1g}^1$ ,  $A_{1g}^2$ , and the in-plane vibrational mode  $E_g^2$  of Bi<sub>2</sub>Se<sub>3</sub> films [16]. Moreover, to explore the possibility of photoactive switching to THz wave, the OTP measurement

used in a ZnTe nonlinear crystal is performed on the Bi<sub>2</sub>Se<sub>3</sub> samples, and the relevant transient THz transmission results are shown in Fig. 2.

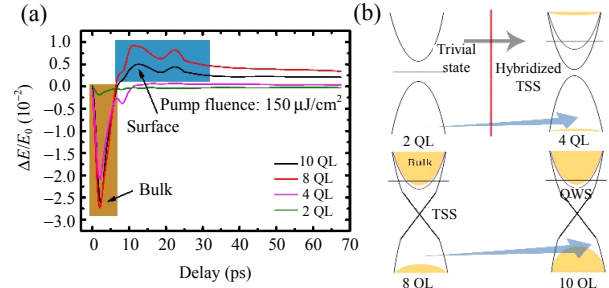


Fig. 2 Thickness-dependent topological phase transition: (a) measured transient THz transmission spectra for the Bi<sub>2</sub>Se<sub>3</sub> samples with different layers (i.e., 2 QL, 4 QL, 8 QL, and 10 QL) showing a double phases recombination process for various time delays and (b) evolution of the band structure of the Bi<sub>2</sub>Se<sub>3</sub> films with an increase in the layer number from 2 QL to 10 QL.

It should be noted that in Fig. 2(a),  $E_0$  and  $E_{\text{Pump}}$  represent the peak values of transmission waveform without and with pump light, respectively, and the pump-induced change in transmission amplitude is denoted as  $\Delta E = E_{\text{Pump}} - E_0$ . Compared with the traditional semiconductors, the TSS of TI makes the time-resolved THz transmission spectra a more complex scenarios instead of an exponential decay process that is proportional to the nonequilibrium carrier density after excitation. Note also that at the time delay of  $\tau = 22$  ps, a peak is observed in  $\Delta E$  curves, which is caused by the back reflection of pump laser on the substrate.

### 3.2 Ultrafast photoinduced response to THz of Bi<sub>2</sub>Se<sub>3</sub> films

During the first several picoseconds ( $\sim 7$  ps),  $\Delta E$  of three Bi<sub>2</sub>Se<sub>3</sub> films (i.e., 4 QL, 8 QL, and 10 QL) is obviously negative, which is presented as a rapid drop in Fig. 2(a). What follows is an increase in THz transmission in 8 QL and 10 QL Bi<sub>2</sub>Se<sub>3</sub> films. Such unusual transparency in 8 QL and 10 QL Bi<sub>2</sub>Se<sub>3</sub> films is attributed to the metallic property of TSS [17]. When an optical pulse approaches, the temperature of the electronic system will rise, with concomitant results of an increased nonequilibrium carrier density and an enhanced scattering rate.

Owing to the metallic TSS property, the impact of the increased scattering rate greatly exceeds the nonequilibrium carrier density in the surface. Thus, after the bulk nonequilibrium carriers survived for the first few picoseconds, the TSS of Bi<sub>2</sub>Se<sub>3</sub> films would possess a stronger and dominant negative photoconductivity, along with the increasing transparency [18].

The vivid topological phase transition is presented in Fig. 2(b), considering several QLs. According to theoretical calculations, 2.5 nm (1 QL  $\approx$  1 nm) is a critical thickness where a phase transition will take place [19]. For 2 QL Bi<sub>2</sub>Se<sub>3</sub> film, which belongs to the two-dimensional (2D) trivial insulator phase, the band structure is similar to an ordinary semiconductor. Thus, only a negligible dip ( $<0.2\%$ ) is observed in the OPTP test of 2 QL film, which can be barely used for THz modulation. Further to that, as illustrated in Fig. 2(b), a stronger bulk state naturally exists in a thicker film resulting in the higher modulation depth in 8 QL and 10 QL films at  $\tau=2.2$  ps. On the other hand, the band gap appears in the surface because of the coupling of boundary modes induced by quantum tunneling [19, 20]. One salient example is the 4 QL film, whose wave functions of two surfaces with opposite spins overlap, leading to the quantum hybridized TSS and the flat  $\Delta E$  curve after  $\tau=10$  ps. It is evident that the band gap would shrink with an increase in the film thickness and completely disappear after 6 QL [21]. In terms of the 8 QL and 10 QL films, their upper and lower band cross each other and form a Dirac cone exhibiting a TSS feature. Therefore, only 8 QL, 10 QL, and thicker Bi<sub>2</sub>Se<sub>3</sub> films can accomplish bi-direction THz switching. Notably, the surface modulation of 8 QL film is better than that of 10 QL film, which is originated from the suppression effect of the surface charged-impurity scattering rate, caused by injected bulk electrons when the temperature is higher than 180 K (Debye temperature) [22].

In order to further support our claims on the photoactive switching of 8 QL Bi<sub>2</sub>Se<sub>3</sub> sample, we carry out temporal THz transmission measurements under various pump conditions, considering two time delays of 2.2 ps (dominated by bulk carriers) and 12.5 ps (dominated by TSS scattering rate), and the corresponding results are presented in Fig. 3. According to the previous discussion, the 8 QL sample responds more effectively to THz wave within 10 ps than the thinner counterparts.

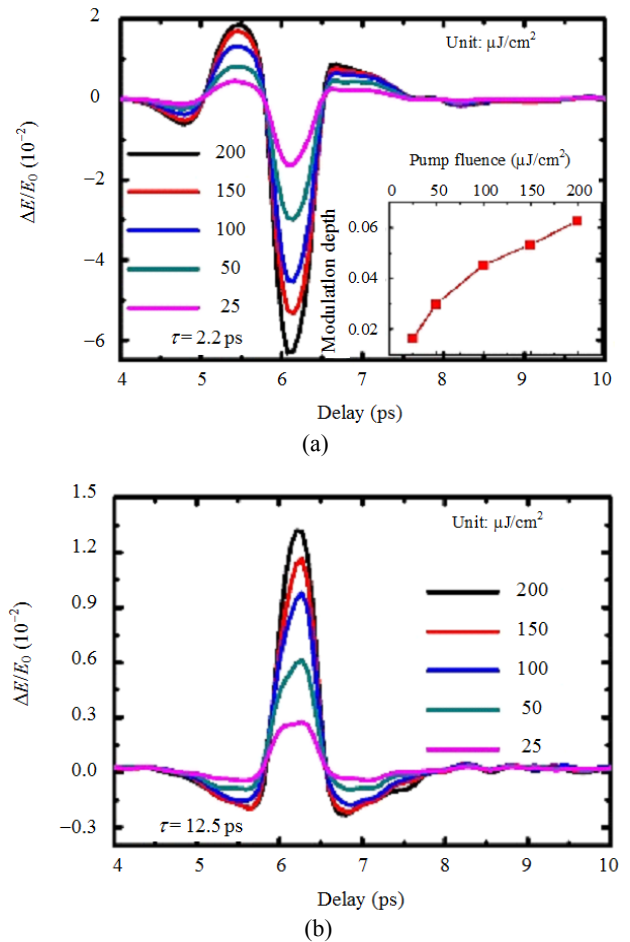


Fig. 3 Measured temporal THz wave transmitted through 8 QL Bi<sub>2</sub>Se<sub>3</sub> sample at the time delay of: (a) 2.2 ps and (b) 12.5 ps, respectively. The inset of (a) is the frequency averaged modulation depth as a function of pump fluence.

From Fig. 3, one can see that the amplitude of temporal THz wave increases with the pump fluence at the time delay  $\tau=2.2$  ps. The frequency averaged modulation depth (defined as the  $|\Delta E / E_0|$ ) approaches its maximum value of 6.4% when pumped with 200  $\mu\text{J}/\text{cm}^2$  laser. Given its ultrathin

thickness of 8 QL  $\text{Bi}_2\text{Se}_3$  ( $\sim 8\text{ nm}$ ) and no additional metal structure, this modulation depth is of great significance even if compared with the perovskite-based photoswitch with the resonance structure, which was recently reported in [23]. According to the inset of Fig. 3(a), the modulation depth is linearly proportional to the pump fluence and not saturated within the measured range, suggesting that the modulation depth can be further enlarged by using a stronger photoexcitation [24]. However, the modulation behavior of  $\text{Bi}_2\text{Se}_3$  at  $\tau = 12.5\text{ ps}$  is comparatively weaker, reaching a modulation depth of 1.3% under  $200\ \mu\text{J}/\text{cm}^2$ . It is worth to mention that most of the reported photoactive THz switches and modulators can only control the transmitted loss of THz wave. In comparison, our  $\text{Bi}_2\text{Se}_3$  sample exhibits the THz modulation in double directions, revealing its potential for furnishing enhanced transmission under pump condition [23, 25].

### 3.3 Ultrafast photoactive THz switching of $\text{Bi}_2\text{Se}_3$ films

For completeness, the frequency-resolved THz transmission spectra are calculated through the fast Fourier transform (FFT) method. It is found from Fig. 4 that THz waves from 0.1 THz to 2.0 THz are effectively modulated, which presents the broadband switching behavior of  $\text{Bi}_2\text{Se}_3$  that may facilitate practical application in the wavelength division multiplexing communication [26]. In the case of  $\tau = 2.2\text{ ps}$  [see Fig. 4(a)], its modulation depth at 0.6 THz region achieves around 7.7%, similar to the frequency averaged results. Additionally, double dips, located at 0.9 THz and 1.9 THz, are deviated from the classical Drude model for transmission spectra shown in Fig. 4. Owing to the band bending near the surface in 4 QL, 8 QL, and 10 QL films, quantum well states (QWSs) are hold as discrete eigenstates as shown in Fig. 2(b). This special quantum state is characterized by a broad dip of THz absorption (at 0.9 THz) in Fig. 4. Furthermore, the

dip at 1.9 THz is attributed to  $\alpha$  optical phonon absorption, and the relevant modulation behavior of  $\text{Bi}_2\text{Se}_3$  is found to be completely suppressed at  $\tau = 2.2\text{ ps}$  ( $< 0.2\%$ ) [19], but approximately 1% modulation depth is achieved at  $\tau = 12.5\text{ ps}$ . Such phenomenon is responsible by the high lattice and electron temperature after pump excitation. During the initial period after light injection, the lattice temperature of the sample is maintained at a relatively high state. At this time, the phonon mode has been all excited by thermal energy, and THz absorption by optical phonon resonance (at  $\sim 1.9\text{ THz}$ ) will be suppressed. This saturation effect will decline with an increase in the time delay, as shown in Figs. 4(a) and 4(b) [27, 28], and the modulation depth at 1.9 THz is related to the lattice temperature. This unique modulation feature provides extra

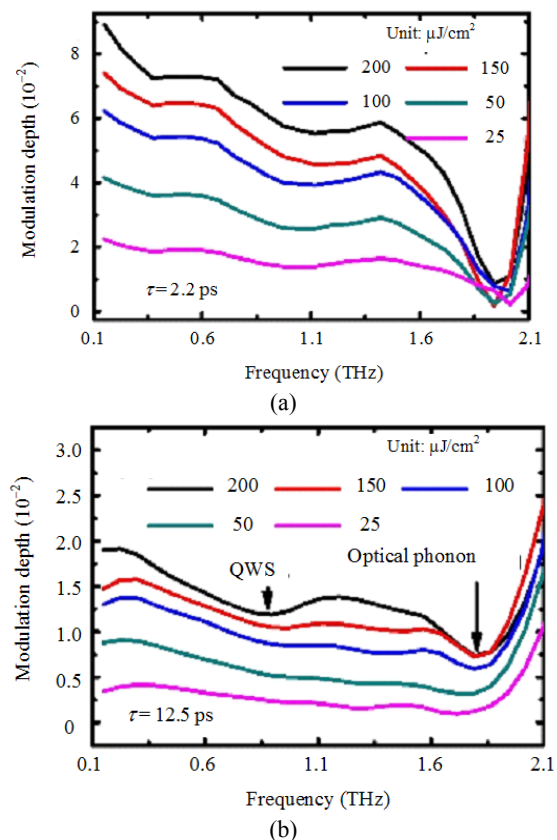


Fig. 4 Corresponding frequency-resolved THz transmission spectra of Fig. 3 at the time delay of: (a) 2.2 ps and (b) 12.5 ps, calculated by the FFT method. Here, two resonant absorption features at 0.9 THz and 1.9 THz are observed, which are caused by the quantum well state (QWS) and optical phonon, respectively.

flexibility in the design of active THz devices with Bi<sub>2</sub>Se<sub>3</sub> films. For convenience of comparing the performances between similar devices, we put Table 1 and list some reported optically controlled THz modulators based on 2D materials whose thickness is parallel to our TIs. The directions of those arrows under the column of “Modulation depth” refer to the modulation effects (increase or decrease) after pumping. Under a similar modulation condition, our sample is found to have comparable modulation depth among these devices with two optional directions.

Table 1 Some optically controlled THz modulators based on 2D material system.

Year	Material	Modulation depth	Modulation bandwidth	Modulation condition	Ref.
2017	GaAs nanowires	13% ↓	0.1 THz–4 THz	800 nm 280 μJ/cm <sup>2</sup>	[29]
2014	Monolayer MoS <sub>2</sub>	30% ↑	0.5 THz–2 THz	400 nm 280 μJ/cm <sup>2</sup>	[30]
2018	Bilayer graphene	1.5% ↑	0.5 THz–2.5 THz	800 nm 340 μJ/cm <sup>2</sup>	[31]
2013	Monolayer graphene	4% ↑	0.5 THz–1.5 THz	800 nm 160 μJ/cm <sup>2</sup>	[32]
2015	Few layer MoS <sub>2</sub>	3.2% ↓	0.5 THz–2.5 THz	800 nm 340 μJ/cm <sup>2</sup>	[33]

Last but not least, our studies also reveal high-speed switching behaviors of these Bi<sub>2</sub>Se<sub>3</sub> films. Unlike some reported photoactive modulators based on the semiconductor substrate (silicon, GaAs, and Ge) whose switching speeds are limited to milliseconds due to their long recombination time, the spatial thermal diffusion mechanisms (i.e., electrons move away from the probed area) of bulk nonequilibrium carriers in the Bi<sub>2</sub>Se<sub>3</sub> sample can be ultrafast switched off and completely recovery for the broadband THz wave within several picoseconds (<5 ps). As presented in Fig. 5(a), the  $\Delta E/E_0$  reaches its minimum value at around 2.6 ps after photoexcitation and then recombines to the zero level within 10 ps. However, in the longer time range [see Fig. 5(b)], where the surface state is dominant, the  $\Delta E/E_0$  increases to its maximum within the delay time of tens picoseconds and then returns to

the steady state within several hundred picoseconds. For simplicity, the exponential function of  $y = ke^{-t/\tau} + y_0$  is adopted to estimate the recombination time of the negative  $\Delta E/E_0$ . Here,  $k$  and  $\tau$  are the ratio coefficient and recombination time, respectively. According to the inset of Fig. 5(a), the bulk state related recombination time is 1.87 ps under the pump fluence of 25 μJ/cm<sup>2</sup> and turns slightly longer ~4.51 ps under a 200 μJ/cm<sup>2</sup> photoexcitation. Hence, it is believed that our Bi<sub>2</sub>Se<sub>3</sub> sample can be switched off within 2.6 ps after photoexcitation and then recombines within 5 ps, verifying the ultrafast switching behavior of TI devices when compared with the recently reported perovskite-metasurface case [23]. Comparatively,

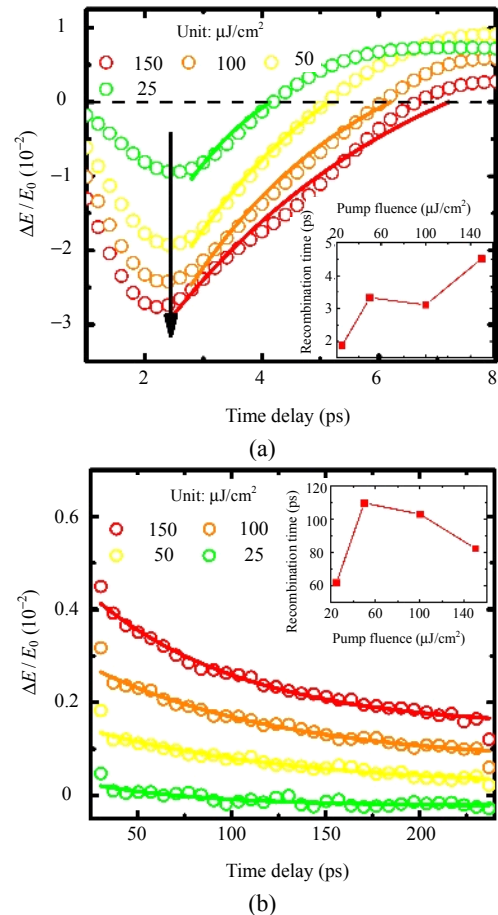


Fig. 5 Excitation dynamics of the 8 QL Bi<sub>2</sub>Se<sub>3</sub> sample with respect to the pump-probe delay dominated by: (a) bulk state (within ~5 ps) and (b) TSS, respectively. The empty circles are experimental results by using the OPTP measurements for various pump fluences. The solid lines are the fitting results of the recombination processes. The insets describe the recombination time as a function of pump fluence.

the recombination process is much longer in the TSS dominated region, which is calculated to be 61.6 ps – 109.7 ps for various pump fluences, showing a graphene-like behavior.

#### 4. Conclusions

In conclusion, we have performed an in-depth study of photoactive switching features for THz wave inside the  $\text{Bi}_2\text{Se}_3$  films. The OPTP measurement reveals that our  $\text{Bi}_2\text{Se}_3$  samples have great potentials for the applications of ultrafast and broadband THz switches. By comparing the OPTP responses of few layers  $\text{Bi}_2\text{Se}_3$  films, it is found that an ultrafast photoactive THz modulation can be completed within 10 ps, corresponding to a modulation speed of 200 GHz, far beyond the speed of other semiconductor-based THz modulators. Such a fast response relies on the spatial hot-electrons diffusion, which is more significant in thinner samples since the reduced diffusion direction makes  $\text{Bi}_2\text{Se}_3$  films suitable for high-speed photo-switches.

Furthermore, by comparison of this time-evolved THz response for both TSS and bulk states of the  $\text{Bi}_2\text{Se}_3$  film, bi-direction modulation and switching of transmitted THz wave are realized by tuning external pump condition. In particular, the 8 QL  $\text{Bi}_2\text{Se}_3$  is proved to be an ideal material for the design of THz photo-switches, with an effective frequency range from 0.1 THz to 2.0 THz and the maximum modulation depth of 7.7%. Our work suggests that excellent properties of  $\text{Bi}_2\text{Se}_3$  films make themselves promising candidates to achieve the effective modulation and switching of THz waves, as well as the application in the low-cost and highly-efficient photoactive and plasmonic devices with versatile functionalities.

#### Acknowledgment

This work was partially supported by Opening Foundation of State Key Laboratory of High Performance Computing (Grant Nos. 201601-01, 201601-02, and 201601-03); Scientific Researches

Foundation of National University of Defense Technology (Grant No. zk16-03-59); Open Research Fund of Hunan Provincial Key Laboratory of High Energy Technology (Grant No. GNJGJS03); Director Fund of State Key Laboratory of Pulsed Power Laser Technology (Grant No. SKL2018ZR05); Opening Foundation of State Key Laboratory of laser and matter interaction (Grant No. SKLLIM1702).

The Opening Foundation of State Key Laboratory of High Performance Computing (Grant Nos. 201601-01, 201601-02, and 201601-03) plays the role of designing the subject and materials growth. The Director Fund of State Key Laboratory of Pulsed Power Laser Technology (Grant No. SKL2018ZR05) and the Opening Foundation of State Key Laboratory of laser and matter interaction (Grant No. SKLLIM1702) play the role of data collection and analysis. The Scientific Researches Foundation of National University of Defense Technology (Grant No. zk16-03-59) and the Open Research Fund of Hunan Provincial Key Laboratory of High Energy Technology (GNJGJS03) play the role of data interpretation and manuscript writing.

**Open Access** This article is distributed under the terms of the Creative Commons Attribution 4.0 International License (<http://creativecommons.org/licenses/by/4.0/>), which permits unrestricted use, distribution, and reproduction in any medium, provided you give appropriate credit to the original author(s) and the source, provide a link to the Creative Commons license, and indicate if changes were made.

#### References

- [1] Y. Ren, R. Wallis, D. S. Jessop, R. D. Innocenti, A. Klimont, H. E. Beere, *et al.*, “Fast terahertz imaging using a quantum cascade amplifier,” *Applied Physics Letters*, 2015, 107: 26–33.
- [2] G. Ducournau, P. Szriftgiser, F. Pavanello, E. Peytavit, M. Zaknoune, D. Bacquet, *et al.*, “THz communications using photonics and electronic devices: the race to data-rate,” *Journal of Infrared, Millimeter and Terahertz Waves*, 2015, 36(2): 198–220.
- [3] M. Theuer, S. S. Harsha, D. Molter, G. Torosyan, and

- R. Beigang, "Terahertz time-domain spectroscopy of gases, liquids, and solids," *Chemphyschem*, 2011, 12(15): 2695–2705.
- [4] C. L. Holloway, A. Dienstfrey, E. F. Kuester, J. F. O. Hara, A. K. Azad, and A. J. Taylor, "A discussion on the interpretation and characterization of metafilms/metasurfaces: the two-dimensional equivalent of metamaterials," *Metamaterials*, 2009, 3(2): 100–112.
- [5] M. Wagner, A. S. Mcleod, S. J. Maddox, Z. Fei, M. Liu, R. D. Averitt, *et al.*, "Ultrafast dynamics of surface plasmons in InAs by time-resolved infrared nanospectroscopy," *Nano Letters*, 2015, 14(8): 4529–4534.
- [6] H. T. Chen, W. J. Padilla, J. M. O. Zide, S. R. Bank, A. C. Gossard, A. J. Taylor, *et al.*, "Ultrafast optical switching of terahertz metamaterials fabricated on ErAs/GaAs nanoisland superlattices," *Optics Letters*, 2007, 32(12): 1620–1622.
- [7] Q. Li, Z. Tian, X. Q. Zhang, R. J. Singh, L. L. Du, J. Q. Gu, *et al.*, "Active graphene-silicon hybrid diode for terahertz waves," *Nature Communications*, 2015, 6: 7082-1–7082-6.
- [8] J. Zhao, Z. J. Xu, Y. Y. Zang, Y. Gong, X. Zheng, K. He, *et al.*, "Thickness-dependent carrier and phonon dynamics of topological insulator Bi<sub>2</sub>Te<sub>3</sub> thin films," *Optics Express*, 2017, 25(13): 14635–14643.
- [9] M. Z. Hasan and C. L. Kane, "Colloquium: topological insulators," *Physics*, 2015, 39(10): 843–846.
- [10] M. Klintenberg, S. Lebegue, M. I. Katsnelson, and O. Eriksson, "A theoretical analysis of the chemical bonding and electronic structure of graphene interacting with Group IA and Group VIIA elements," *Physical Review B: Condensed Matter*, 2010, 81: 085433-1–085433-5.
- [11] P. P. Di, M. Ortolani, O. Limaj, G. A. Di, V. Giliberti, F. Giorgianni, *et al.*, "Observation of Dirac plasmons in a topological insulator," *Nature Nanotechnology*, 2013, 8(8): 556–560.
- [12] M. Autore, F. D. Apuzzo, A. D. Gaspare, V. Giliberti, O. Limaj, P. Roy, *et al.*, "Plasmon-phonon interactions in topological insulator microrings," *Advanced Optical Materials*, 2015, 3(9): 1257–1263.
- [13] L. V. Yashina, J. Sánchezbarriga, M. R. Scholz, A. A. Volykhov, A. P. Sirotnina, S. N. Vera, *et al.*, "Negligible surface reactivity of topological insulators Bi<sub>2</sub>Se<sub>3</sub> and Bi<sub>2</sub>Te<sub>3</sub> towards oxygen and water," *ACS Nano*, 2013, 7(6): 5181–5191.
- [14] Y. Okada and V. Madhavan, "Topological insulators: plasmons at the surface," *Nature Nanotechnology*, 2013, 8(8): 541–542.
- [15] J. A. Sobota, S. Yang, J. G. Analytis, Y. L. Chen, I. R. Fisher, P. S. Kirchmann, *et al.*, "Ultrafast optical excitation of a persistent surface-state population in the topological insulator Bi<sub>2</sub>Se<sub>3</sub>," *Physical Review Letters*, 2012, 108(11): 117403-1–117403-5.
- [16] K. M. F. Shahil, M. Z. Hossain, V. Goyal, and A. A. Balandin, "Micro-Raman spectroscopy of mechanically exfoliated few-quintuple layers of Bi<sub>2</sub>Te<sub>3</sub>, Bi<sub>2</sub>Se<sub>3</sub>, and Sb<sub>2</sub>Te<sub>3</sub> materials," *Journal of Applied Physics*, 2012, 111(5): 054305-1–054305-8.
- [17] B. C. Park, T. H. Kim, K. I. Sim, B. Kang, J. W. Kim, B. Cho, *et al.*, "Terahertz single conductance quantum and topological phase transitions in topological insulator Bi<sub>2</sub>Se<sub>3</sub> ultrathin films," *Nature Communications*, 2015, 6: 6552-1–6552-8.
- [18] R. V. Aguilar, J. Qi, A. J. Taylor, D. A. Yarotski, R. P. Prasankumar, M. Brahlek, *et al.*, "Time-resolved terahertz dynamics in thin films of the topological insulator Bi<sub>2</sub>Se<sub>3</sub>," *Applied Physics Letters*, 2015, 106(1): 011901-1–011901-5.
- [19] C. X. Liu, H. J. Zhang, B. Yan, X. L. Qi, T. Frauenheim, X. Dai, *et al.*, "Oscillatory crossover from two dimensional to three dimensional topological insulators," *Physical Review B: Condensed Matter*, 2009, 81(4): 1–8.
- [20] J. Linder, "Anomalous finite size effects on surface states in the topological insulator Bi<sub>2</sub>Se<sub>3</sub>," *Physical Review B: Condensed Matter*, 2009, 80(20): 2665–2668.
- [21] Y. Zhang, K. He, C. Z. Chang, C. L. Song, L. L. Wang, X. Chen, *et al.*, "Crossover of the three-dimensional topological insulator Bi<sub>2</sub>Se<sub>3</sub> to the two-dimensional limit," *Nature Physics*, 2009, 6(8): 712–712.
- [22] A. Crepaldi, F. Cilento, B. Ressel, C. Cacho, J. C. Johannsen, M. Zacchigna, *et al.*, "Evidence of reduced surface electron-phonon scattering in the conduction band of Bi<sub>2</sub>Se<sub>3</sub> by non-equilibrium ARPES," *Physical Review B: Condensed Matter*, 2013, 88(12): 95–103.
- [23] M. Manjappa, Y. K. Srivastava, A. Solanki, A. Kumar, T. C. Sum, and R. Singh, "Hybrid lead halide perovskites for ultrasensitive photoactive switching in terahertz metamaterial devices," *Advanced Materials*, 2017, 29(32): 1605881-1–1605881-6.
- [24] D. S. Yang, T. Jiang, and X. A. Cheng, "Optically controlled terahertz modulator by liquid-exfoliated multilayer WS<sub>2</sub> nanosheets," *Optics Express*, 2017, 25(14): 16364–16377.
- [25] X. K. Liu, Z. Y. Zhang, X. Lin, K. L. Zhang, Z. M. Jin, Z. X. Cheng, *et al.*, "Terahertz broadband modulation in a biased BiFeO<sub>3</sub>/Si heterojunction," *Optics Express*, 2016, 24(23): 26618–26628.
- [26] S. Punthawanunt, S. Soysouvanh, K. Luangxaysana, S. Mitatha, M. Yoshida, N. Komine, *et al.*, "THz switching generation using a PANDA ring resonator for high speed computer communication," in *Proceeding of Progress In Electromagnetics Research Symposium Proceedings*, KL, Malaysia,

- 2012, pp. 173–176.
- [27] Y. H. Wang, D. Hsieh, E. J. Sie, H. Steinberg, D. R. Gardner, Y. S. Lee, *et al.*, “Measurement of intrinsic dirac fermion cooling on the surface of the topological insulator  $\text{Bi}_2\text{Se}_3$  using time-resolved and angle-resolved photoemission spectroscopy,” *Physical Review Letters*, 2012, 109(12): 127401-1–127401-5.
- [28] S. Sim, M. Brahlek, N. Koirala, S. Cha, S. Oh, and H. Choi, “Ultrafast terahertz dynamics of hot Dirac-electron surface scattering in the topological insulator  $\text{Bi}_2\text{Se}_3$ ,” *Physical Review B*, 2014, 89(16): 165137-1–165137-8.
- [29] S. A. Baig, J. L. Boland, D. A. Damry, and H. H. Tan, “An ultrafast switchable terahertz polarization modulator based on III–V semiconductor nanowires,” *Nano Letters*, 2017, 17: 2603–2610.
- [30] C. H. Lui, A. J. Frenzel, D. V. Pilon, Y. H. Lee, and X. Ling, “Trion-induced negative photoconductivity in monolayer  $\text{MoS}_2$ ,” *Physical Review Letters*, 2014, 113(16): 166801-1–166801-14.
- [31] S. Kar, V. L. Nguyen, D. R. Mohapatra, and Y. H. Lee, “Ultrafast spectral photoresponse of bilayer graphene: optical pump-terahertz probe spectroscopy,” *ACS Nano*, 2018, 12(2): 1785–1792.
- [32] G. Jnawali, Y. Rao, H. Yan, and T. F. Heinz, “Observation of a transient decrease in terahertz conductivity of single-layer graphene induced by ultrafast optical excitation,” *Nano Letters*, 2013, 13(2): 524–530.
- [33] S. Kar, Y. M. Su, R. R. Nair, and A. K. Sood, “Probing photo-excited carriers in a few layer  $\text{MoS}_2$  laminate by time resolved optical pump-terahertz probe spectroscopy,” *ACS Nano*, 2015, 9(12): 12004–12010.